Journal of Molecular Spectroscopy 395 (2023) 111792

Contents lists available at ScienceDirect

Journal of Molecular Spectroscopy

journal homepage: www.elsevier.com/locate/yjmsp

Article

# The molecular oxygen 118-GHz line intensity revision

Dmitriy S. Makarov *, Evgeniy A. Serov, Tatyana A. Galanina, Aleksandra O. Koroleva, Mikhail Yu. Tretyakov

*IAP RAS, 46 Ulyanov Str., 603950 Nizhny Novgorod, Russia*

ARTICLE INFO

*Keywords:*
Microwave spectroscopy
Molecular oxygen
Collisional coupling
Line intensity
Speed dependent effects
Atmospheric absorption

ABSTRACT

The intensity of the atmospheric diagnostic fine-structure line of the $O_2$ molecule at 118.75 GHz is revised based on multiple measurements with a resonator spectrometer in pure $O_2$ and $O_2$–$N_2$ mixture at pressures ranging from 250 to 1500 Torr and temperatures within 278–327 K. The resulting intensity of $1.000(3)\cdot10^{-25}$ cm/molec confirms the earlier measurements and allows decreasing the uncertainty down to ~0.3%. An excellent agreement with the result of calculations presented in HITRAN is demonstrated, suggesting that the 10%–20% uncertainty recommended by the database for all fine structure lines is too large.

## 1. Introduction

The millimeter-wave spectrum of molecular oxygen is an important object for remote sensing of the atmosphere. In particular, the single fine-structure line of the oxygen molecule at 118 GHz is used to retrieve temperature and pressure profiles of the Earth's atmosphere [1]. Being the transition between two lowest energy levels of the molecule, this line is also important for astrophysical studies and is successfully detected in molecular clouds [2].

The uncertainty of spectral line parameters is known to extend to the uncertainty of remote sensing retrievals. The shape of the line under atmospheric conditions is well studied, including accounting for the speed-dependence and line mixing effects. The parameters of the speed-dependent half-width [3,4], as well as central frequency and its pressure-shifting coefficient [5] are measured with high accuracy. As shown in [6], not only the uncertainties of the line shape parameters themselves but also their covariations are essential. The same study points out that the intensities of molecular oxygen fine-structure line are the parameters whose variation within the uncertainty interval $\sigma$ leads to a noticeable change in the brightness temperature in the frequency intervals where absorption due to oxygen is significant. The dominating impact of intensity uncertainty on predicted absorption was also shown in [7].

It is worth recalling that the integrated line intensity at a given temperature is determined by molecular parameters (such as dipole moment, transition frequency, lower level energy, degeneracy factor and partition sum). At a specified pressure, the area under the line is the product of the integrated intensity and the number of absorbing molecules. The integrated intensity does not depend on line shape profile and may be calculated *ab initio*. The state-of-the-art high accuracy quantum chemistry methods allow reaching an agreement with measurements at the level of 0.01% [8]. To the best of our knowledge, similar calculations have not been performed for molecular oxygen lines. The current intensities used in the propagation models are obtained on the basis of effective Hamiltonians and the corresponding empirical data. The uncertainty provided in HITRAN is about 10% [9], although the real accuracy is likely to be much better [7,10]. The most precise (with a stated uncertainty of 0.4%) earlier measurements of the 118-GHz line intensity are based only on a few recordings of the line profile [3] at room temperature and require confirmation.

This study is devoted to the refinement of the 118-GHz line intensity value on the basis on a larger amount of experimental observations at temperatures ranging from 278 up to 327 K. Note that the results of this work can be important not only for the remote sensing applications utilizing this particular line, but also for refining the absorption model of the molecular oxygen 60-GHz band, which is also widely used for the retrieval of atmospheric parameters. The band consists of lines of the same nature but corresponding to different rotational quantum numbers. The dependence of line intensity on quantum numbers is known; therefore, the 118-GHz line data can serve as a calibration point for all other lines of the band.

The paper is organized as follows. The experimental details are briefly described in Section 2. Section 3 presents the method of experimental data treatment. The obtained results are discussed in Section 4.

* Corresponding author.
*E-mail address:* dmak@ipfran.ru (D.S. Makarov).

https://doi.org/10.1016/j.jms.2023.111792
Received 16 March 2023; Received in revised form 18 May 2023; Accepted 21 May 2023
Available online 26 May 2023

**Table 1**
Details of the experimental conditions.

| Temperature, K | Gas | Pressure range, Torr | Number of recordings |
|---|---|---|---|
| 278.5 | $O_2$ | 500–1500 | 9 |
| 297.0 | $O_2$ | 250–1500 | 8 |
| 297.5 | $O_2$+$N_2$[a] | 750–1500 | 8 |
| 317.5 | $O_2$ | 500–1500 | 9 |
| 326.0 | $O_2$ | 750–1250 | 3 |

[a]Typical value of $O_2$ pressure is 750 Torr

## 2. Experiment

Recordings of the line profile were obtained using the resonator spectrometer [11]. The oxygen and nitrogen samples with a specified purity better than 99.999% were purchased from a local supplier. The experimental conditions adopted for this study are given in Table 1. Raw experimental data were acquired and processed using a conventional, well-documented procedure (see [3,11–13] and references therein). The absorption coefficient was obtained on the basis of the difference of the resonator curve half-widths measured when the resonator was filled with the studied and a non-absorbing gas, respectively. To decrease the influence of standing waves and the related interference pattern on the obtained spectra, measurements were carried out several times at several predetermined positions of the waveguide system relative to the resonator and averaged.

The chamber was equipped with a set of thermal sensors placed on both mirrors and in the free space along the resonator. As follows from the sensor readings, the difference in the gas temperature from one mirror to the other was up to 3 K at the ends of the experimental temperature range, which was taken into account as described below. The variation of the temperature readings from each sensor did not exceed 0.5 K.

## 3. Data treatment

The absorption corresponding to the neighboring lines was removed prior to treating the experimental spectra. The most significant contribution under the studied line is given by the 60-GHz band wing. The absorption was calculated using the Millimeter-wave Propagation Model (MPM) [14] adapted for pure oxygen and its arbitrary mixtures with nitrogen [7,15] and subtracted from the recorded spectra.

As a line shape fitting model, we adopted the quadratic speed-dependent Van Vleck–Weisskopf profile with line mixing (usually referred to as the qSDVVWLM profile), which was used in our earlier studies [3,4]:

$$SDVVWLM(\nu) = S\frac{1}{\pi}\left(\frac{\nu}{\nu_0}\right)^2 \int_0^\infty \left(\frac{\Gamma(z)+Y\cdot(\nu-\nu_0)}{\Gamma(z)^2+(\nu-\nu_0)^2} + \frac{\Gamma(z)-Y\cdot(\nu+\nu_0)}{\Gamma(z)^2+(\nu+\nu_0)^2}\right) f_{MB}(z)dz \quad (1)$$

In this expression, $S$ is line intensity, $\nu_0$ is central frequency, $\Gamma$ is speed-dependent half-width, $Y$ is first-order (in pressure) mixing parameter and $f_{MB}(z)$ is Maxwell–Boltzmann distribution. We consider the quadratic dependence of half-width on speed: $\Gamma(z) = \Gamma_0 + \Gamma_2 \cdot (z^2 - 1.5)$, where $z = \upsilon/\upsilon_m$ is reduced speed, with $\upsilon$ and $\upsilon_m$ being active molecule speed and its most probable speed, respectively. The mixing parameter may generally be considered as speed-dependent with its own quadratic dependence [12], but even for the case of a highly pronounced mixing effect in the oxygen spectrum, the impact of this speed-dependence lies far beyond the sensitivity of the spectrometer [16]. To account for the imperfections of the 60-GHz band wing subtraction and baseline accounting, a linear versus frequency polynomial was added to the line shape model function.

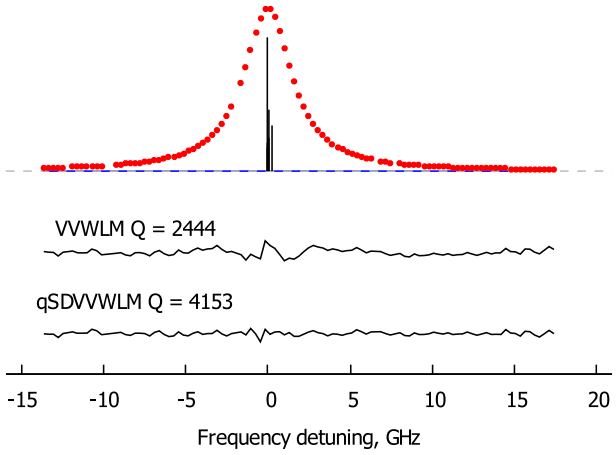


**Fig. 1.** Residuals of the VVWLM and qSDVVWLM profiles fitted to the experimental recordings at 278.5 K and 750.56 Torr. The red points correspond to the measured absorption, the gray dashed line shows the zero level, the blue solid line shows the contribution of the additive linear function (see the text for details). The black stems show the positions of the studied line for the ground and excited vibrational state of different $O_2$ isotopologues, their relative intensities are given on logarithmic scale. The residuals are scaled up to the factor of 50 for better visibility. Q is the fit quality index. Frequency detuning is from the line central frequency value.

**Table 2**
Values of fixed line shape coefficients (speed-averaged collisional broadening $\gamma_0$, broadening speed-dependence $\gamma_2$, their temperature dependence exponents $n$ and central frequency $\nu_0$) measured by RAD spectrometer [4,5].

| Parameter | $O_2$, MHz/Torr | $n_{O_2}$ | $N_2$, MHz/Torr | $n_{N_2}$ |
|---|---|---|---|---|
| $\gamma_0$ | 2.272(6) | 0.776(6) | 2.296(2) | 0.774(8) |
| $\gamma_2$ | 0.173(3) | 0.68(15) | 0.174(4) | 0.774(8) |
| $\nu_0$ (MHz) | 11 8750.3328(8) | | | |

The results of the model (1) fit to the experimental recording at a chosen pressure and temperature,[1] compared to the use of a similarly constructed model profile based on the speed-independent Van Vleck–Weisskopf profile with line mixing (VVWLM profile), are shown in Fig. 1 justifying the choice of the model. For quantitative evaluation, the fit quality index (marked "Q" in this figure and hereinafter) is calculated as the maximum absorption to the residual standard deviation ratio.

The multifit procedure was used to retrieve line intensity from experimental spectra. The line shape model was fitted to several recordings simultaneously taking into account the expected pressure and temperature dependence of collisional parameters of the line shape model and line intensity:

$$X(P,T) = x(T_0)\cdot P\cdot\left(\frac{T_0}{T}\right)^{n_x}, \quad (2)$$

where $X$ is the collisional parameter value at given pressure $P$ and temperature $T$, $x$ is the corresponding coefficient, $T_0$ is reference temperature (296 K in our case), and $n_x$ is the $T$-dependence exponent for the considered parameter.

For the line area under certain conditions, we used the well-known equation:

$$I(P,T) = I_0(T_0)\frac{P}{k_B T}\frac{Q(T_0)}{Q(T)}\frac{exp(-c_2 E_{low}/T)}{exp(-c_2 E_{low}/T_0)}\frac{1-exp(-c_2\nu_0/T)}{1-exp(-c_2\nu_0/T_0)}, \quad (3)$$

[1] Each recording was obtained by averaging several profiles recorded under constant conditions with different positions of the waveguide system, as described in Section 2.

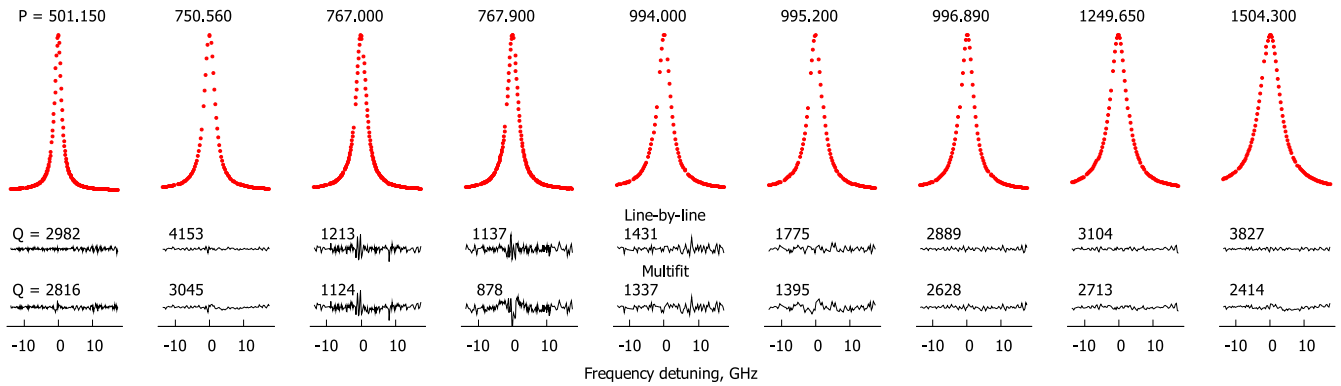


**Fig. 2.** Recordings in pure oxygen at 278.5 K and residuals of the fitted model profile (1) given by line-by-line fit and multifit. Oxygen pressures are specified above each profile.

where $I_0(T_0)$ is the integrated intensity value at the reference temperature, $E_{low}$ is the energy of the lower level of the transition, $Q(T)$ is partition sum (data from HITRAN [9] were used), and $c_2 = hc/k_B$ = 1.4387769 cm·K.

The multifit procedure allows reducing potential systematic errors in the retrieved data due to the correlation between multiple variable parameters of the model. In principle, the procedure can be applied to all experimental recordings. However, the quality of recordings made under different experimental conditions, including potential systematic distortion of experimental data, is somewhat different. Under these conditions, it is not clear how to choose the corresponding weight of recording in the fitting procedure. For convenience of experimental data treatment and transparency of further analyses of the obtained information, the recordings were grouped into batches corresponding to a certain temperature.

Note that the line intensity and width are anti-correlated in the fitting procedure, which may lead to systematic misestimation of both parameters. To avoid this problem and further reduce line intensity uncertainty we decided to fix the collisional broadening coefficients $\gamma_0$ and $\gamma_2$ (both for self- and $N_2$-broadening) and their temperature exponents to the values reported recently in the work [4]. The line center frequency was fixed to the value reported in [5]. The values of the fixed parameters and their temperature dependence exponents are given in Table 2. The normalized line intensity, pressure shifting coefficients, mixing coefficients and parameters of the additive polynomial were adjusted parameters of the model function.

Fig. 2 shows typical residuals of fitting the model to the experimental data on the example of the batch of recordings corresponding to 278.5 K. For comparison, the residuals of fitting all parameters of the model to each recording separately are also given in the figure, demonstrating expected minor imperfections of the multifit residuals, which are usually attributed to the inaccuracy of pressure and temperature sensor readings and experimental systematics. Nevertheless, for most recordings the decrease of the fit quality is insignificant, about 20% on the average.

In total, 37 intensity values normalized to the $O_2$ concentration and recalculated to $T_0$ = 296 K were obtained from the spectra. For the studied gas pressures, the considered line profile ($^{16}O_2$ isotopologue in the fundamental vibrational and electronic states) overlaps with the profiles corresponding to the same fine structure transition in the excited vibrational state and to other $O_2$ isotopologues. Due to the large line width and insignificant frequency difference (see the spectrum diagram in Fig. 1), the resulting profile can be safely considered as a single line with a somewhat higher intensity. Five weak lines with the relative strength ranging from $10^{-3}$ to $10^{-4}$ from the studied one were taken into account using the HITRAN [9] data. Their joint contribution to the observed line intensity (about $0.003–0.002 \cdot 10^{-25}$ cm/molec depending on temperature) was subtracted from the values obtained from the fit. Thus, the result was the intensity of the $N = 1-$ line of the main $O_2$ isotopologue in the ground state in natural abundance. The obtained results are shown in Fig. 3 plotted versus the concentration of $O_2$ molecules.

**Table 3**
Error budget of the uncertainty value.

| Statistical uncertainty, % | Pressure uncertainty, % | Temperature uncertainty, % | Total uncertainty, % |
|---|---|---|---|
| 0.2 | 0.2 | 0.1 | 0.3 |

The line mixing coefficient $y$ retrieved from the experimental data can be used for cross-checking. The value corresponding to the reference temperature of 296 K is −4.804(35) 1/Torr, which is in a fairly good agreement with −4.71(3) 1/Torr reported earlier in [3].

## 4. Results and discussion

The total amount of measurements is quite significant but still insufficient to make a correct statistical analysis. To improve the estimation of the mean measured value and its confidence interval evaluation, the bootstrapping method was applied [17]. Within this approach, pseudo-sets are generated by random picking of the values from the initial data set. Then, an average value is calculated for each pseudo-set. The resulting averaged pseudo-set values are arranged in ascending order. The median value corresponds to the expected value, while half the distance between the 2.5% and 97.5% interquantile distance (i.e. the range of 95% of the analyzed values around the median point) corresponds to the expected statistical uncertainty. In our case, the size of the pseudo-set was 37 (the size of the bootstrapped data set), and the number of iterations (i.e. the generated pseudo-sets) was 10000, which makes possible variations negligible due to random picking. The confidence interval obtained from this procedure corresponds to the statistical uncertainty only. It is worth noting that this uncertainty value is less than a standard deviation calculated from the original data, as bootstrapping effectively increases the weight of the points near the averaged value and decreases one of the most outlying points. The assumption of normal distribution of the results leads to a conclusion that outliers are less probable.

The total error budget also includes uncertainties of pressure and temperature sensors, which were taken into account as independent error sources (see Table 3). The resulting value is shown in Fig. 3, together with the total uncertainty with solid and dashed red lines, respectively.

Two sources of possible systematic errors in the obtained values were considered. The first one is temperature gradients in the used vertical configuration of the Fabry–Perot resonator chamber. To evaluate the impact of the gradient, the optical depth of one radiation passage from the lower mirror to the upper mirror was modeled. The absorption profile was calculated by integration along the path (by

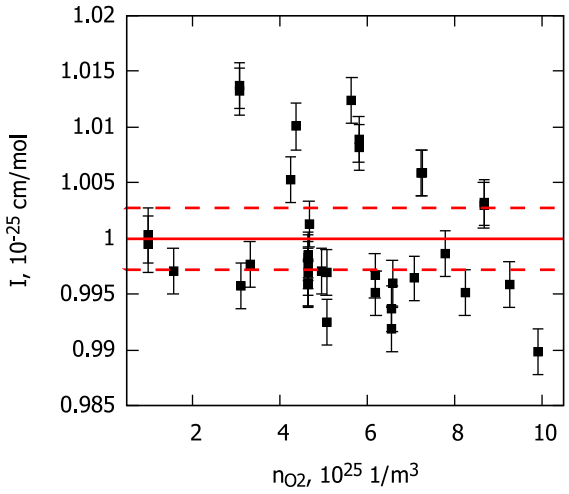


**Fig. 3.** All values of 118-GHz line intensity measured in this study versus oxygen molecules concentration. Error bars for the points are total uncertainties (see Table 3). Solid horizontal and dashed lines are for the mean measured value (exactly coinciding with HITRAN's value) and its total uncertainty.

analogy with atmospheric absorption profile calculation for the vertical radiometric trace), assuming a linear change of the gas temperature inside the chamber. The relative difference between this profile and a similar profile for the mean homogeneous temperature did not exceed $10^{-4}$. This difference is several times lower than the instrumental noise level and therefore unable to produce noticeable bias.

The second source is a limited frequency interval used for line profile recordings. The interval is specified by the operating frequency range of the radiation source. For this reason the low frequency wing of the line profile is cut more than the high frequency one, which is more pronounced at higher pressures (Fig. 2). Recall that we have a limited signal to noise ratio and use the non-ideal line shape model. Under these conditions, the asymmetry of the recorded profile may become a problem. Numerical modeling of the profile with symmetrical and non-symmetrical location of the line center within the operating frequency range has shown that the systematic misevaluation of the intensity is indeed present and increases with increasing pressure (i.e. with progressive cutting of one wing of the line). However, the magnitude of this effect under our experimental conditions should not exceed 0.1% and, thereby, can be neglected.

The resulting value of the line integrated intensity is $1.000(3)\cdot10^{-25}$ cm/molec which is in exact agreement with the current HITRAN value. The obtained value also agrees within uncertainty limits with $0.993(4)\cdot10^{-25}$ cm/molec reported in our previous study [3] on the basis of the analysis of four experimental profiles recorded at room temperature. At the same time, the value from the JPL catalogue is $1.002\cdot10^{-25}$ cm/molec, which is greater but still within the experimental uncertainty range.

It is worth noting that the statistical uncertainty of the intensity value retrieved from the model fitting to a single experimental profile is near 0.02%, which is one order of magnitude less than the statistical uncertainty of the value obtained over all measurements. At the same time, the measured intensity values are scattered within ±1%. This result is in agreement with the intensity measurements of the R(0) and R(1) lines of CO molecule in CO–Ar mixtures [12] performed with the same instrument. This indicates that the uncertainty of the used pressure gauge (which can be reduced by a factor of 4 if we had another model of the sensor) is not dominating in the error budget. The major factor limiting a further increase in intensity measurement accuracy is uncontrolled experimental noise, including slow-scale instabilities.

To conclude, let us recap our findings. Our experimental study confirmed the subpercent uncertainty of the integrated intensity of the N=1- line of molecular oxygen widely used for the remote sensing of the atmosphere. The obtained value is significantly more reliable than the previous result due to the extended statistical data based on multiple measurements under various experimental conditions and treatment using the bootstrapping method. The excellent agreement of the obtained value with the HITRAN data suggests a similar agreement (as discussed in detail in [7]) for other fine-structure $O_2$ lines forming the 60-GHz band, which is also used for atmospheric applications. Our measurements confirm that the uncertainties currently provided for this line in HITRAN can be substantially reduced from 10%–20% (uncertainty index "4") to less than 1% (uncertainty index "8").

## CRediT authorship contribution statement

**Dmitriy S. Makarov:** Conceptualization, Methodology, Software, Writing – original draft. **Evgeniy A. Serov:** Funding acquisition, Investigation, Data curation. **Tatyana A. Galanina:** Investigation, Data curation, Resources. **Aleksandra O. Koroleva:** Investigation, Data curation, Validation. **Mikhail Yu. Tretyakov:** Supervision, Writing – review & editing.

## Declaration of competing interest

The authors declare that they have no known competing financial interests or personal relationships that could have appeared to influence the work reported in this paper.

## Data availability

Data will be made available on request.

## Acknowledgments

The experiments were carried out using the Large-scale research facilities "CKP-7" (USU №3589084). The study was supported by the Russian Science Foundation (project No. 18–72–10113, https://rscf.ru/en/project/18-72-10113/).

## References

[1] V. Wulfmeyer, R.M. Hardesty, D.D. Turner, A. Behrendt, M.P. Cadeddu, P. Di Girolamo, P. Schlüssel, J. Van Baelen, F. Zus, A review of the remote sensing of lower tropospheric thermodynamic profiles and its indispensable role for the understanding and the simulation of water and energy cycles, Rev. Geophys. 53 (3) (2015) 819–895.

[2] B. Larsson, R. Liseau, L. Pagani, P. Bergman, P. Bernath, N. Biver, J.H. Black, R.S. Booth, V. Buat, J. Crovisier, C.L. Curry, M. Dahlgren, P.J. Encrenaz, E. Falgarone, P.A. Feldman, M. Fich, H.G. Florén, M. Fredrixon, U. Frisk, G.F. Gahm, M. Gerin, M. Hagstrom, J. Harju, T. Hasegawa, A. Hjalmarson, L.E.B. Johansson, K. Justtanont, A. Klotz, E. Kyrola, S. Kwok, A. Lecacheux, T. Liljestrom, E.J. Llewellyn, S. Lundin, G. Megie, G.F. Mitchell, D. Murtagh, L.H. Nordh, L.-A. Nyman, M. Olberg, A.O.H. Olofsson, G. Olofsson, H. Olofsson, G. Persson, R. Plume, H. Rickman, I. Ristorcelli, G. Rydbeck, A.A. Sandqvist, F.V. Scheele, G. Serra, S. Torchinsky, N.F. Tothill, K. Volk, T. Wiklind, C.D. Wilson, A. Winnberg, G. Witt, Molecular oxygen in the ophiuchi cloud, Astron. Astrophys. 466 (3) (2007) 999–1003.

[3] M.A. Koshelev, T. Delahaye, E.A. Serov, I.N. Vilkov, C. Boulet, M.Y. Tretyakov, Accurate modeling of the diagnostic 118-GHz oxygen line for remote sensing of the atmosphere, J. Quant. Spectrosc. Radiat. Transfer 196 (2017) 78–86.

[4] M.A. Koshelev, I.N. Vilkov, T.A. Galanina, E.A. Serov, D.S. Makarov, M.Y. Tretyakov, Temperature behavior of collisional parameters of oxygen fine-structure lines: $O_2$–$O_2$ case, J. Quant. Spectrosc. Radiat. Transfer 298 (2023) 108493.

[5] M.A. Koshelev, G.Y. Golubiatnikov, I.N. Vilkov, M.Y. Tretyakov, Molecular oxygen fine structure with sub-kHz accuracy, J. Quant. Spectrosc. Radiat. Transfer 278 (2022) 108001.

[6] D. Cimini, P.W. Rosenkranz, M.Y. Tretyakov, M.A. Koshelev, F. Romano, Uncertainty of atmospheric microwave absorption model: impact on ground-based radiometer simulations and retrievals, Atmos. Chem. Phys. 18 (20) (2018) 15231–15259.

[7] D.S. Makarov, M.Y. Tretyakov, P.W. Rosenkranz, Revision of the 60-GHz atmospheric oxygen absorption band models for practical use, J. Quant. Spectrosc. Radiat. Transfer 243 (2020) 106798.

[8] K. Bielska, A.A. Kyuberis, Z.D. Reed, G. Li, A. Cygan, R. Ciuryło, E.M. Adkins, L. Lodi, N.F. Zobov, V. Ebert, D. Lisak, J.T. Hodges, J. Tennyson, O.L. Polyansky, Subpromille measurements and calculations of CO (3–0) overtone line intensities, Phys. Rev. Lett. 129 (2022) 043002.

[9] I.E. Gordon, L.S. Rothman, R.J. Hargreaves, R. Hashemi, E.V. Karlovets, F.M. Skinner, E.K. Conway, C. Hill, R.V. Kochanov, Y. Tan, P. Wcisło, A.A. Finenko, K. Nelson, P.F. Bernath, M. Birk, V. Boudon, A. Campargue, K.V. Chance, A. Coustenis, B.J. Drouin, J.-M. Flaud, R.R. Gamache, J.T. Hodges, D. Jacquemart, E.J. Mlawer, A.V. Nikitin, V.I. Perevalov, M. Rotger, J. Tennyson, G.C. Toon, H. Tran, V.G. Tyuterev, E.M. Adkins, A. Baker, A. Barbe, E. Canè, A.G. Császár, A. Dudaryonok, O. Egorov, A.J. Fleisher, H. Fleurbaey, A. Foltynowicz, T. Furtenbacher, J.J. Harrison, J.M. Hartmann, V.M. Horneman, X. Huang, T. Karman, J. Karns, S. Kassi, I. Kleiner, V. Kofman, F. Kwabia-Tchana, N. Lavrentieva, T. Lee, D. Long, A. Lukashevskaya, O. Lyulin, V. Makhnev, W. Matt, S. Massie, M. Melosso, S. Mikhailenko, D. Mondelain, H. Müller, O. Naumenko, A. Perrin, O. Polyansky, E. Raddaoui, P. Raston, Z. Reed, M. Rey, C. Richard, R. Tóbiás, I. Sadiek, D. Schwenke, E. Starikova, K. Sung, F. Tamassia, S. Tashkun, J. Vander Auwera, I. Vasilenko, A. Vigasin, G. Villanueva, B. Vispoel, G. Wagner, A. Yachmenev, S. Yurchenko, The HITRAN2020 molecular spectroscopic database, J. Quant. Spectrosc. Radiat. Transfer 277 (2022) 107949.

[10] M. Toureille, S. Béguier, T. Odintsova, M. Tretyakov, O. Pirali, A. Campargue, The $O_2$ far-infrared absorption spectrum between 50 and 170 $cm^{-1}$, J. Quant. Spectrosc. Radiat. Transfer 242 (2020) 106709.

[11] M.A. Koshelev, I.I. Leonov, E.A. Serov, A.I. Chernova, A.A. Balashov, G.M. Bubnov, A.F. Andriyanov, A.P. Shkaev, V.V. Parshin, A.F. Krupnov, M.Y. Tretyakov, New frontiers in modern resonator spectroscopy, IEEE Trans. Terahertz Sci. Technol. 8 (2018) 773–783.

[12] M.Y. Tretyakov, E.A. Serov, D.S. Makarov, I.N. Vilkov, G.Y. Golubiatnikov, T.A. Galanina, M.A. Koshelev, A.A. Balashov, A.A. Simonova, F. Thibault, Pure rotational R(0) and R(1) lines of CO in Ar baths: experimental broadening, shifting and mixing parameters in a wide pressure range versus ab initio calculations, Phys. Chem. Chem. Phys. 25 (2023) 1310–1330.

[13] E.A. Serov, N. Stolarczyk, D.S. Makarov, I.N. Vilkov, G.Y. Golubiatnikov, A.A. Balashov, M.A. Koshelev, P. Wcisło, F. Thibault, M.Y. Tretyakov, CO–Ar collisions: ab initio model matches experimental spectra at a sub percent level over a wide pressure range, J. Quant. Spectrosc. Radiat. Transfer 272 (2021) 107807.

[14] P. Rosenkranz, Line-by-line microwave radiative transfer (non-scattering), URL http://cetemps.aquila.infn.it/mwrnet/lblmrt_ns.html.

[15] M.Y. Tretyakov, M.A. Koshelev, V.V. Dorovskikh, D.S. Makarov, P.W. Rosenkranz, 60-GHz oxygen band: precise broadening and central frequencies of fine structure lines, absolute absorption profile at atmospheric pressure, revision of mixing coefficients, J. Molec. Spectrosc. 231 (2005) 1–14.

[16] M.A. Koshelev, I.N. Vilkov, D.S. Makarov, M.Y. Tretyakov, P.W. Rosenkranz, Speed-dependent broadening of the $o_2$ fine-structure lines, J. Quant. Spectrosc. Radiat. Transfer 264 (2021) 107546.

[17] URL https://en.wikipedia.org/wiki/Bootstrapping_(statistics).